Healable Capacitive Touch Screen Sensors Based on Transparent Composite Electrodes Comprising Silver Nanowires and a Furan/Maleimide Diels–Alder Cycloaddition Polymer

Junpeng Li,[†,‡,§] Jiajie Liang,[†,§] Lu Li,[†] Fengbo Ren,[⊥] Wei Hu,[†] Juan Li,[†] Shuhua Qi,[‡] and Qibing Pei*[,†]

[†]Department of Materials Science and Engineering, Henry Samueli School of Engineering and Applied Science, University of California, Los Angeles, California 90095, United States, [‡]Department of Applied Chemistry, School of Science, Northwestern Polytechnical University, Xi'an Shaanxi 710072, China, and [⊥]Department of Electrical Engineering, Henry Samueli School of Engineering and Applied Science, University of California, Los Angeles California 90095, United States. [§]J. Li and J. Liang contributed equally to this work.

ABSTRACT

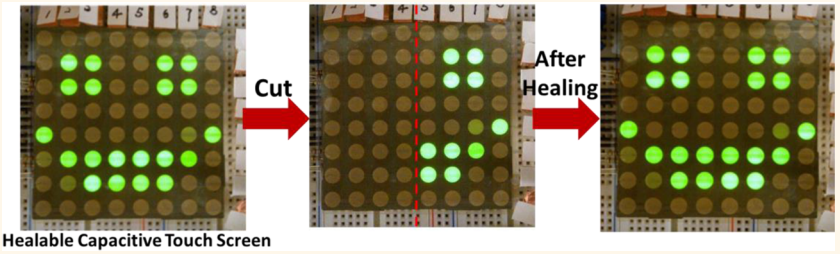

A healable transparent capacitive touch screen sensor has been fabricated based on a healable silver nanowire–polymer composite electrode. The composite electrode features a layer of silver nanowire percolation network embedded into the surface layer of a polymer substrate comprising an ultrathin soldering polymer layer to confine the nanowires to the surface of a healable Diels–Alder cycloaddition copolymer and to attain low contact resistance between the nanowires. The composite electrode has a figure-of-merit sheet resistance of 18 Ω/sq with 80% transmittance at 550 nm. A surface crack cut on the conductive surface with 18 Ω is healed by heating at 100 °C, and the sheet resistance recovers to 21 Ω in 6 min. A healable touch screen sensor with an array of 8 × 8 capacitive sensing points is prepared by stacking two composite films patterned with 8 rows and 8 columns of coupling electrodes at 90° angle. After deliberate damage, the coupling electrodes recover touch sensing function upon heating at 80 °C for 30 s. A capacitive touch screen based on Arduino is demonstrated capable of performing quick recovery from malfunction caused by a razor blade cutting. After four cycles of cutting and healing, the sensor array remains functional.

KEYWORDS: capacitive touch sensor · transparent composite electrode · self-healing · silver nanowire

Mobile devices such as mobile phones, tablets and laptop computers have become ubiquitous in our daily lives and work places. Capacitive touch screen is widely used on these mobile devices for its intuitive user interface, high sensitivity, multitouch capability, and working stability. The capacitive touch sensor monitors the change in capacitance at the point on the screen where a finger is placed, and recognizes the touch position. The most common material used to form the touch sensor is indium tin oxide (ITO) coating on glass or on polyethylene terephthalate (PET) film. As a ceramic, ITO makes the touch screen sensor brittle and easily damaged.[1,2] Crack formation on ITO/glass or ITO/PET touch screens happens rather commonly due to accidental drop or scratching, which affects aesthetics, usability, and even results in device malfunction. Replacing the ITO-based touch sensor with a mechanically and electrically healable material would improve the reliability of the touch sensor and extend device lifetime. To date, considerable efforts have been made to fabricate various healable or self-healing materials with the aim of fault-tolerant,[3] longer-lasting electronic devices[4,5] and recyclability.[6]

* Address correspondence to qpei@seas.ucla.edu.

Received for review November 20, 2014 and accepted December 8, 2014.

Published online December 08, 2014
10.1021/nn506610p

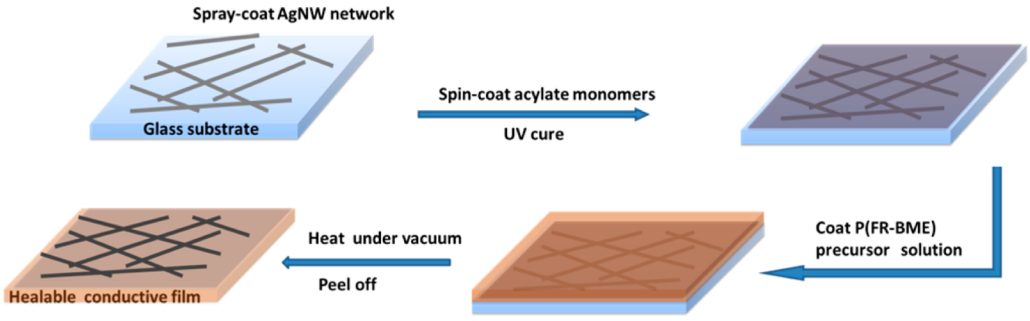

Figure 1. Schematic illustration of the fabrication of a healable conductive film. The thicknesses of acrylate coating after UV curing, and P(FR-BME) were 70 nm and 150 μm, respectively.

However, to the best of the authors' knowledge, there has been no report of a healable or self-healing material applied for touch sensor.

So far, the most studied self-healing material is the single-healing composite comprising microcapsules of healing agents. Upon crack intrusion and the rupture of microcapsules, healing agents are released and cured.[7,8] Conductive material based on this approach would lack visual transparency. Materials based on reversible chemical bonding are capable of multiple self-healing or mending.[4,9−13] However, for applications in thin film electronic devices such as the touch sensors, being solid state and healing in dry atmosphere would be appreciated for compactness and to avoid circuit shortage. In this regard, polymers based on the reversible Diels−Alder (DA) cycloaddition reaction are particularly attractive thanks to being fully solid state and capable of multiple damage-healing simply by heating at fairly low temperature.[4,9−14] The most frequently used healable DA system is the furan/maleimide pair.[9,15,16−20] We have recently reported a healable semitransparent conductor based on a composite of silver nanowires (AgNWs) and a furan/maleimide DA copolymer substrate.[21] The visual transparency is insufficient for touch screen sensor application. The challenge stems from the conflicting requirements of low coating density of AgNW for visual transparency and high density such that the AgNWs can contact and reform the percolation network when the damaged DA polymer substrate is healed.

Herein, we report the fabrication of a highly transparent and healable composite electrode by employing an ultrathin soldering layer on a DA polymer substrate. An AgNW percolation network is embedded in the soldering layer for high surface conductivity. Such a soldering layer is effective to lower the sheet resistance of the transparent composite electrode, and more importantly, to facilitate the recovery of surface conductivity as the damaged electrode is healed by heating. The resulting composite electrode allows the demonstration of capacitive touch screen sensors that can recover capacitive sensing function by heating at 80 °C for 30 s with a hair dryer.

RESULTS AND DISCUSSION

A transparent and healable copolymer (P(FR-BME)) was synthesized through a reversible DA cycloaddition reaction of two cross-coupling comonomers, a furan oligomer (FR) and 1,8-bis(maleimido)-1-ethylpropane (BME) whose chemical structures are shown in Supporting Information Figure S1. The optical images in Supporting Information Figure S2 demonstrate the mendability of this copolymer by heating at 100 °C.

The acrylate monomers consisting of a polyester acrylate (PA) and furfuryl methacrylate (FM) form a ultrathin layer copolymer (P(PA-FM)) after UV curing in the healable conductive film. Figure 1 illustrates the fabrication of a healable transparent conductive film. The process begins with spray-coating AgNW on a release glass substrate, followed by spin-coating a solution of 5 wt % concentration in cyclopentanone, which comprises PA and FM at a weight ratio of 4:1 (See support information for details). A FR and BME comonomer solution (P(FR-BME) precursor) is deposited and cured at 70 °C under vacuum for 6 h to form the self-healing substrate. The resulting composite film is peeled off the release glass substrate. AgNW percolation network is transferred into the ultrathin intermediate P(PA-FM) layer bonded on the surface of the P(FR-BME) substrate.

PA in the ultrathin P(PA-FM) is a multifunctional oligomer with excellent wetting property on AgNW. FM possesses a methacrylate on one end and a furfuryl on the other end. The vinyl groups in these two comonomers can be copolymerized under UV to form a cross-linked polymer network. A DA chemical bonding is formed between furfuryl groups of P(PA-FM), and maleimide groups of P(FR-BME) to promote interface bonding strength. (See Figure S4 and further discussion below)

A AgNW-P(FR-BME) composite electrode without employing a P(PA-FM) layer is fabricated and characterized using SEM. During the curing of P(FR-BME), the preformed AgNW network on glass is immersing in the precursor solution with low viscosity for 6 h. The nanowires could relocate due to thermodynamics or Brownian motion. Even small movement could

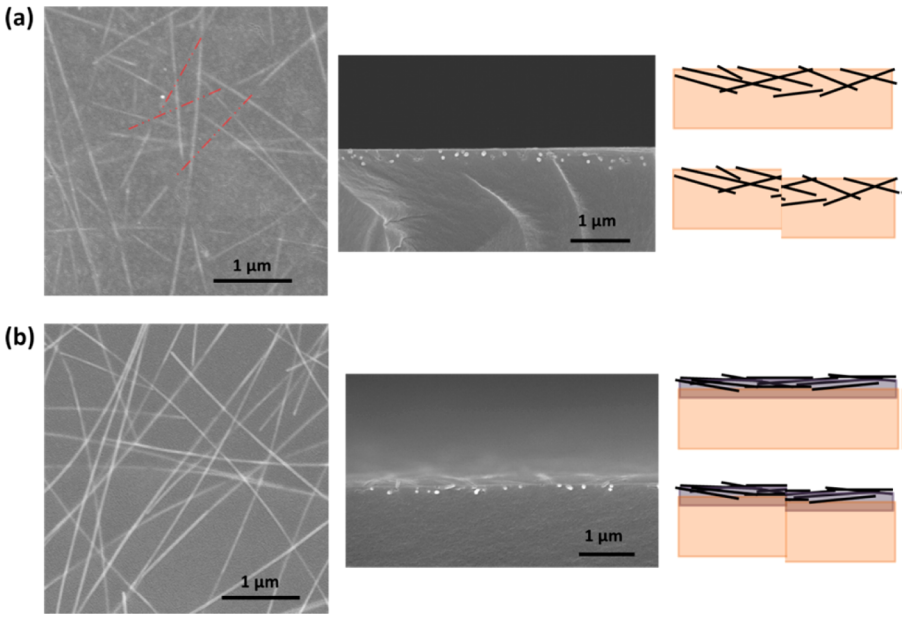

Figure 2. Distribution of AgNWs in a surface of healable P(FR-BME) polymer substrate without an ultrathin P(PA-FM) layer (a) and with an ultrathin P(PA-FM) layer (b). (a) SEM image of AgNW embedded in P(FR-BME) polymer film (*left*). Red dash lines track nanowires going inside the polymer matrix. SEM image of the cross-section of the composite (*middle*). Illustration of AgNW in P(FR-BME) polymer substrate and reconnection after cutting-healing cycle (*right*). (b) SEM images and illustration of the composite electrode comprising the ultrathin P(PA-FM) layer.

cause the nanowires to partially detach from the glass substrate and distribute deeper into polymer matrix. As displayed in Figure 2a, segments of the nanowires submerge into the P(FR-BME), and the AgNW network distributes in a layer about 200 nm thick as shown in the cross-sectional image. Therefore, the conductivity of this composite is low. Such undesirable motion of the nanowires could take place not only during curing but also during the healing at elevated temperature when the polymer matrix is rendered low viscosity. As a result, the surface conductivity would diminish.

Adding an ultrathin P(PA-FM) layer in the composite electrode helps "solder" the AgNW network together and shields it from intrusion by the healable mixture during curing and healing. The P(PA-FM) network remains a rigid, cross-linked network during the curing and healing of the DA copolymer. AgNW embedded in this intermediate layer cannot move in the P(PA-FM) network. As shown in Figure 2b, the ultrathin P(PA-FM) layer can gather AgNW together along substrate surface. This helps to achieve a better conductivity than that of the composite without P(PA-FM) layer. For instance, by transferring the same coating density of AgNWs from glass substrate, the composite electrode comprising the ultrathin P(PA-FM) layer has a sheet resistance of 18 Ω/sq. The composite electrode without this intermediate layer shows a sheet resistance of 310 Ω/sq (see data in Supporting Information Figure S3).

During healing of the composite electrode at an elevated temperature, the DA copolymer is rendered low viscosity, and the top surface separated by a cut damage fuses together to resume a low total surface area. As a result, the ultrathin P(PA-FM) layer from the separated halves is brought together, and the AgNW percolation network is reconnected. The enrichment of AgNW along the surface benefits restoration of the surface conductivity during healing; even a slight mismatch would not significantly deter the restoration as shown in the illustration. The improvement is shown in Figure S3 where the composite electrode with the P(PA-FM) layer had a restored sheet resistance of 22 Ω/sq (the original film was 18 Ω/sq). In comparison, the sheet resistance of composite electrode without the P(PA-FM) layer became 896 Ω/sq, almost three times higher than the original value.

In the remaining discussions, we will focus on the composite electrodes with ultrathin P(PA-FM) layers, and all composite electrodes hereafter refer to this architecture. The robustness of this composite electrode is also demonstrated in Figure S4. After 1000 cycles of repeated adhesion and peeling with a 3 M Scotch tape, the sheet resistance increased only 1 Ω/sq, indicative of a strong mechanical bonding between AgNW network and P(PA-FM), and between P(PA-FM) and P(FR-BME) as well.

As shown in Figure 3a, the transmittances at 550 nm are 89%, 80% and 75% for P(FR-BME) pure polymer film, its composite films with 18 Ω/sq and 6.2 Ω/sq, respectively. The visual transparency of the 18 Ω/sq composite film is comparable to the commercial ITO-PET film with 35 Ω/sq sheet resistance.

The healability of the composite electrode after razor blade cutting was examined by measuring the

recovery of the resistance of the electrode during heating (Figure 4a). The cut penetrated into the polymer substrate by roughly 40 μm depth. For a film with an original resistance of 18 Ω, after cutting across the surface, its resistance increased to infinity (cannot be measured by a multimeter). After the film was heated at 100 °C for 6 min, its resistance dropped to 21 $\pm$ 1 Ω indicating AgNW reconnection (see Supporting Information Figure S5). Further recovery could be obtained with additional heating time. The recovery speed at 80 C was slightly lower; after healing for 8 min, the resistance recovered to 22 $\pm$ 2 Ω. Healing processes of composite electrodes with various sheet resistances are shown in Supporting Information Figure S6. Composite film with low sheet resistance has high probability of AgNW reconnection during healing, which contributes largely to conductive recovery. Additionally, conductive healing efficiency relies on cutting depth shown in Supporting Information Figure S7. Composite film with shallow cutting would perform high healing efficiency due to low surface tension. Supporting Information Figure S8 shows the mechanical healing performance. In 6 min, the mechanical healing efficiency reaches 97%.

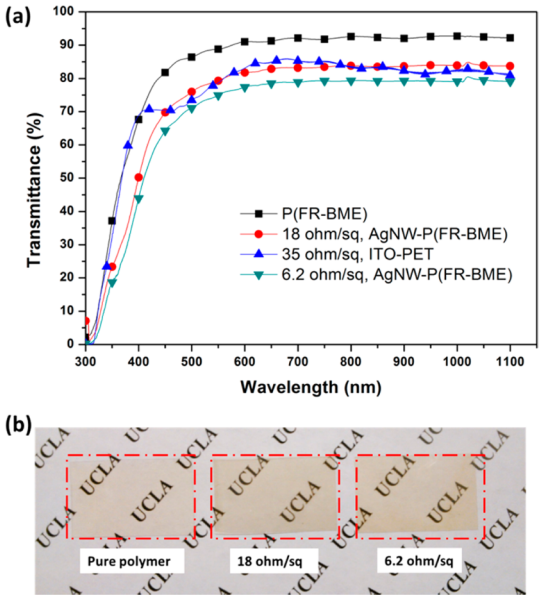

Figure 3. (a) Transmittance spectra of P(FR-BME) film, two AgNW-P(FR-BME) composite electrodes with different sheet resistances. Data for a commercial ITO-PET film is also shown for comparison. All transmittance data are inclusive of substrate. The thickness of all films is 150 μm. (b) Optical photographs of P(FR-BME) polymer film and composite films.

To evaluate the robustness of the healed films, a film with a resistance recovered to 22 Ω was repeatedly bent to a diameter of 5 mm for 1000 cycles. A gradual increase of the resistance was observed; however, the total increase was only 6.8% after the 1000 cycles of bending (Figure 4b). The healing can be repeated at the same location for multiple times as shown in Figure 4c. The resistance of a composite conductor with initial resistance of 18 Ω increased to an infinite value after each cutting. The resistance recovered to 21, 60, and 700 Ω after healing at 100 °C in 6 min after the first, second, and third cutting, respectively. This declining healing efficiency in repeated cutting-healing at the location is considered to be caused by the difficulty for the AgNW/P(PA-FM) layer to reconnect during healing of the substrate.

A capacitive touch sensing film was prepared as illustrated in Figure 5a. An AgNW percolation network was spray-coated on a release glass substrate through a shadow mask. A monomer solution of P(PA-FM) was spin coated onto the AgNW coating and then UV curing. A layer of a solution of FR and BME in

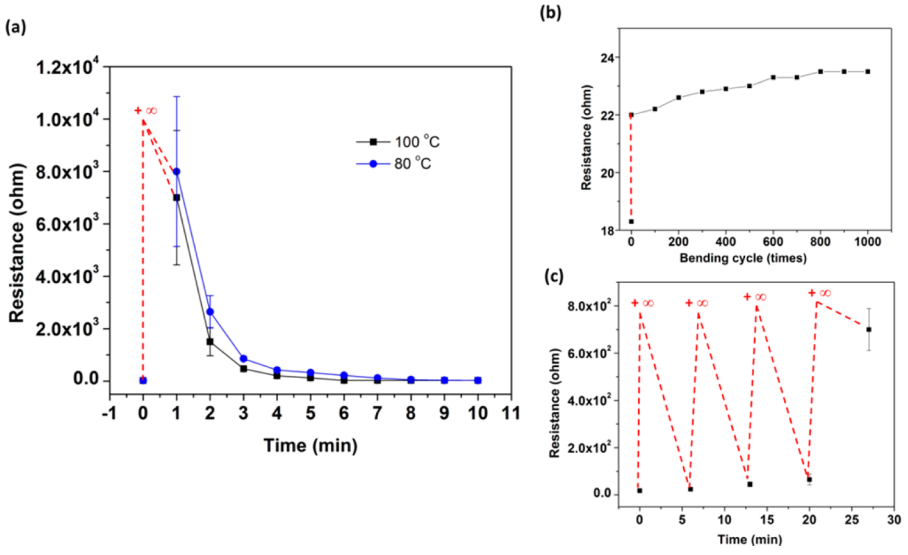

Figure 4. (a) Measured transient resistance of composite electrodes with 18 Ω during healing process at 100 and 80 °C. (b) A 1000 cycles of bending to 5 mm diameter, and (c) multiple-healing cycles at the same location at 100 °C. All samples (20 mm × 20 mm) with sheet resistance of 18 Ω/sq.

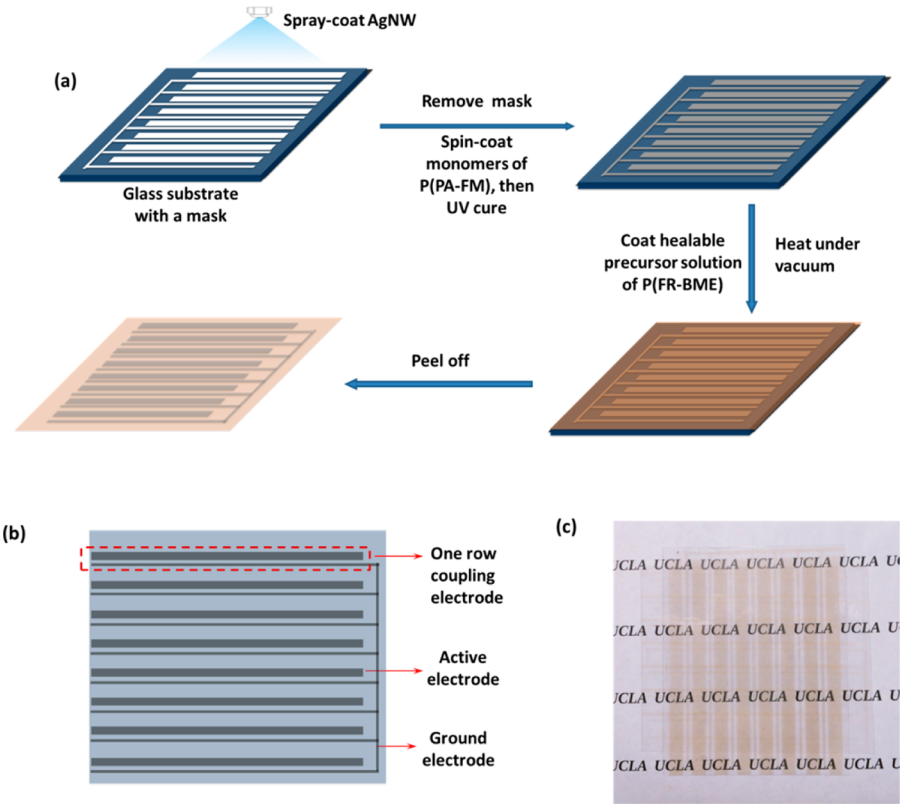

Figure 5. (a) Process flow to fabricate a patterned composite film for capacitive touch screen sensor. (b) Schematic illustration of a composite film patterned as the row electrodes. (c) Optical photograph of a transparent touch sensor fabricated by laminating two composite films patterned as row and column electrodes, respectively, with the conductive surface of the column electrodes facing the nonconductive surface of the row electrodes. Both films have the same dimension of 60 mm × 80 mm × 0.18 mm and sheet resistance of 18 Ω/sq in the electrode areas.

cyclopentanone, was drop-cast and heated in vacuum to form healable polymer film.

The touch sensing pattern, as shown in Figure 5b, was defined by the shadow mask. Each composite film has 8 alternating active electrodes and a ground electrode. An active electrode couples with a neighboring ground electrode to form a capacitor. The capacitance is measured with an input potential. Figure 5c presents photograph of a touch sensor comprising two capacitive sensing films stacked together to form the touch sensing circuitry with 8 × 8 independently controlled sensor pixels. The UCLA logo can be clearly seen through the stacked touch sensor films. This touch sensor as a basic model of most commercial products has X-Y coordinate to determine the touch location when cooperation with a corresponding controller firmware.

Figure 6a,b illustrates the touch sensing mechanism of this circuitry. When a finger touches a couple of electrodes, capacitances (C_f) between finger and target electrodes are generated. In the meantime, system capacitance increases to C_t.

As an *RC* circuitry, the time constant (τ) is an indicator of charging time and working stability, expressed as,

$$\tau = R \times C \quad (1)$$

τ is the time required to charge a capacitor, through a resistor, by ≈63.2% of the difference between the initial potential and final potential, which contributes greatly to the swift performance of a capacitive touch sensor. *R* and *C*, respectively, represent the resistance and capacitance along the circuitry.

To adjust sensitivity and stability, an extra resistor (R_e) of 1 M Ω is placed in series with the coupling electrodes. Resistance (*R*) should be,

$$R = R_g + R_a + R_e \quad (2)$$

C_s and C_t represent system capacitance when standby or touching.

System capacitance (C_s and C_t), electrode resistance ($R_g + R_a$) and time constant (τ) during cutting-healing process are shown in Figure 6c. The coupling electrodes with initial resistance of 3100 Ω could sense 43 ± 0.9 and 231 ± 6 pF when standby and touching, respectively. The time constant changed accordingly. After cutting along the red dash line, the touch area became separated from the system. Electrode resistance increased to a large value beyond measurable range of a multimeter. A slightly lower capacitance than standby status was measured due to shorter coupling electrodes. No capacitive response was measured even touching. During healing, the electrode resistance ($R_g + R_a$) along the *RC* circuitry decreased

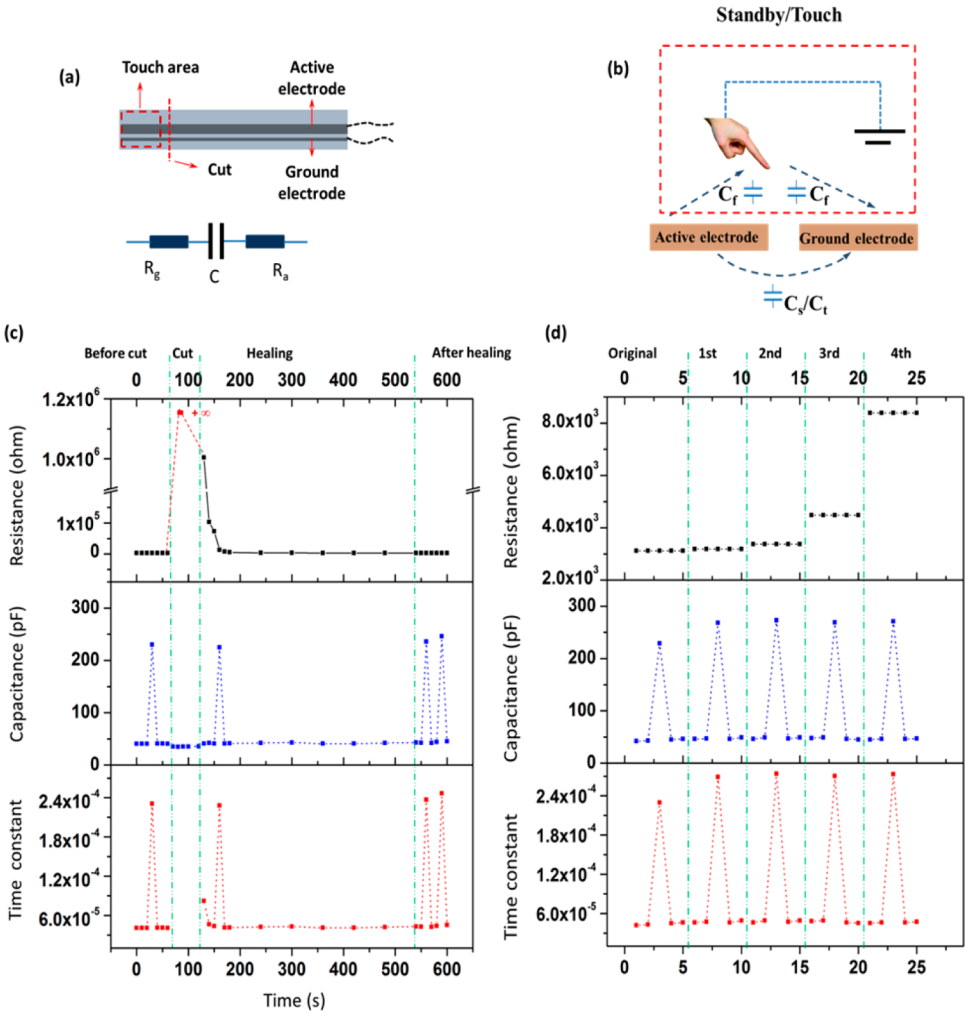

Figure 6. (a) Sketch of a couple of row active electrode and ground electrode connected to external control circuitry. R_g, R_a and C in RC circuitry diagram represent resistances of ground electrode, active electrode, and system capacitance of a couple of electrodes. One touch sensing area with a size of 1/8 of the entire coupling electrodes, marked in a red rectangle, is separated due to deliberate cut damage along the red dash line. (b) The electric field and capacitance during a finger approaching the coupling electrodes. C_s and C_t represent system capacitance when standby and touching, respectively. (c) Electrode resistance ($R_g + R_a$), system capacitance (C_s and C_t) and time constant of a couple of electrodes *versus* time during cutting-healing (healing at 80 °C) process. (d) Changes of electrode resistance ($R_g + R_a$), system capacitance (C_s and C_t) and time constant of a couple of electrodes after specified cycles of cutting-healing (healing at 80 °C).

dramatically, and the capacitance restored to the standby and responded properly.

To be applied as a touch screen sensor, healing temperature should be as low as possible to avoid damaging heat-sensitive electronic components. The healing temperature was set as 80 °C. The row coupling electrodes recovered capacitive sensing in 30 s (Figure 6c). After 8 min heating time, the *RC* circuitry recovered to its original value.

Figure 6d presents multiple-healing performance of the touch sensor. The electrode resistance ($R_g + R_a$) after each successive healing was 3189, 3376, 4486, and 8393 Ω, respectively. The capacitance changed a little, as did the time constant. The coupling electrodes could work properly for a touch screen sensor circuitry.

A couple of column electrodes with a resistance of 2700 Ω could also sense 55 ± 2 and 266 ± 18 pF when standby and touching, respectively, and recovered capacitive sensing in 30 s at 80 °C. τ was largely unchanged after four cycles of cutting-healing, indicative of high working stability surviving multiple cutting (shown in Supporting Information Figure S10).

To demonstrate the application of the healable touch sensors in practical devices, a capacitive touch screen sensor was made by stacking row electrodes and column electrodes at 90° angle to form an array of 8 × 8 capacitive touch sensing points, each point being formed at an overlap of coupling row and column electrodes (Figure 7a). The touch locations can be determined though the capacitance changes, on both a row electrode and a column electrode, as shown in Figure 7b. The capacitive touch screen sensor was applied on an Arduino-based touch screen control system.

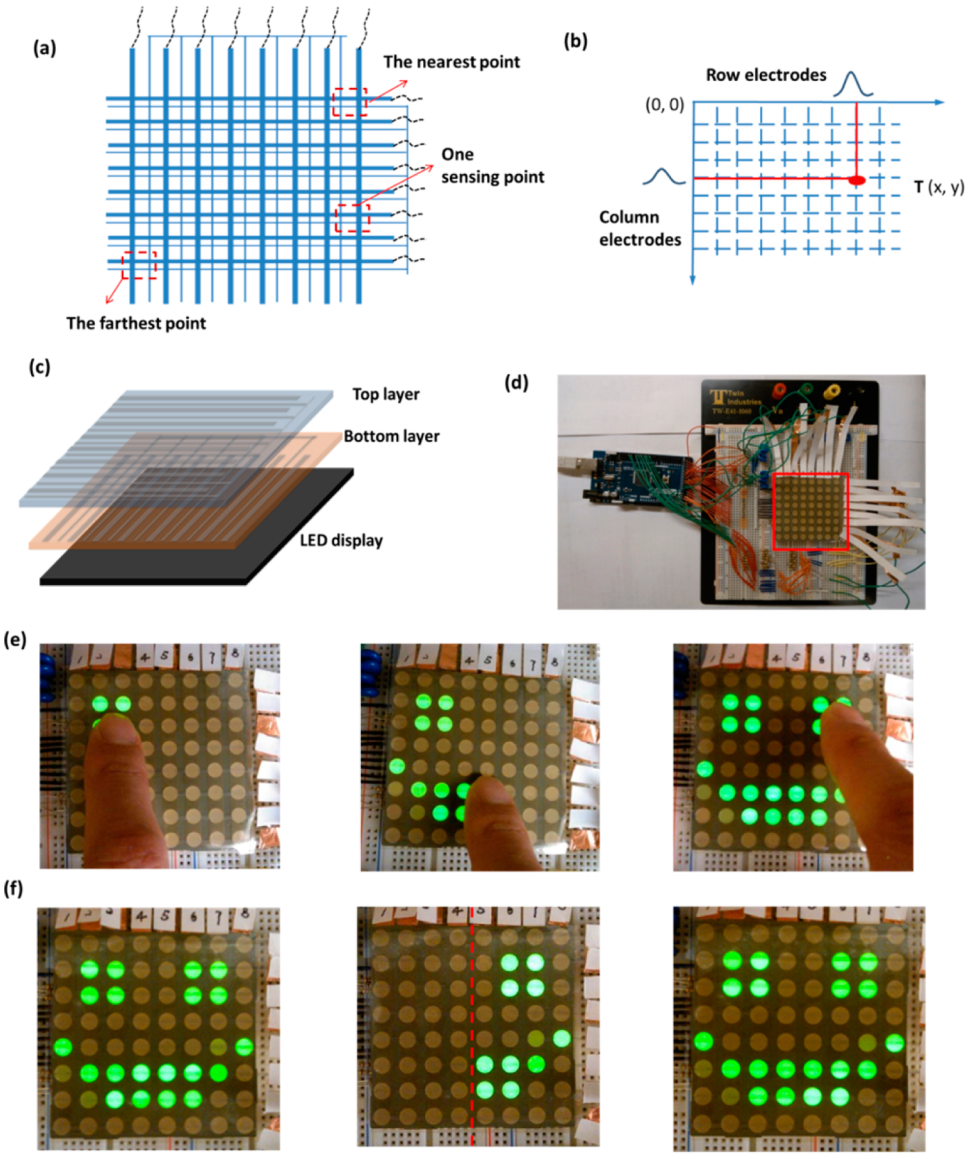

Figure 7. (a) Schematic of row electrodes and column electrodes stacked at 90° angle. (b) A touch point is located by capacitive changes across a row electrode on top film and a column electrode on bottom film. (c) Illustration of two capacitive sensing films, overlaid on a LED display, with conductive AgNW network in the upper surface of each sensing film. (d) Photograph showing the entire capacitive touch screen system. Eight ×8 LED display is connected to a programmable control board Arduino Mega 2560, which is powered by a USB cable. Two touch sensing films are overlaid on the LED panel. The overlaps of coupling row and coupling column electrodes are upright over individual LEDs. Copper foils are attached to the ends of the sensing electrodes for contacts with external electronics. The red rectangle indicates the location of the sensing films and LED panel. (e) and (f) Snapshots from a Supplementary video clip showing the operation and healing of the touch screen. A smiley face is drawn on the touch screen (e). (f) Demonstration of the healing of the touch screen. Before cutting, a smiley face can be drawn on the touch screen (*left*). Cut along the red dash line, and only one-half of the smiley face can be drawn (*middle*). After healing at 80 °C for 30 s with a hair drier, the entire smiley face can be drawn again (*right*).

Arduino is a microcontroller capable of applying 5 V as a step input to a resistor and a capacitor in series and measuring the time required for the potential on the capacitor to reach 2 V.[22] Upon a finger touch, system capacitance switches from C_s to C_t, which requires additional charging time with an input potential applied. This touch screen system can detect a time change in the charging state of a couple of electrodes relative to a fixed threshold. If both charging times of a row electrode and a column electrode are detectable, an LED pixel below the overlap is turned on. As the finger leaves the electrodes, a calibration is carried out to reset the microcontroller for the next detection.

Response time, defined as the elapsed time to charge the system capacitor in the RC circuitry, can be expressed as

$$t = RC \ln[V_u/(V_u - V_t)] \quad (3)$$

Where V_u and V_t are the input potential and the potential on the capacitor at time t, respectively.

When reaching 2 V in response to a step input of 5 V, the response time has the following relationship with *RC*,

$$t = RC \ln(5/3) \quad (4)$$

or, equivalently,

$$t = \tau \times 0.51 \quad (5)$$

The response time of a couple of electrodes when touching can be calculated by eq 5.

The longer response time of a couple of row electrodes and a couple of column electrodes would be the response time of a sensing point, which is confirmed by the same row electrode and column electrode. The response times of the nearest sensing point with lowest resistance and the farthest sensing point with highest resistance are 134 and 146 μs, respectively (shown in Supporting Information Table S1).

The supplementary video clip demonstrates the touching function of the sensor by drawing a smiley face on the LED array and the healing of the damaged sensor by heating with a hair drier. Snapshots in Figure 7e show a smiley face drawn on the touch screen with a fingertip. The snapshots demonstrating the healing function are displayed in Figure 7f. To mimic physical damage during practical use, a razor blade cut along the red dash line between the fourth column electrode and the fifth column electrode was made to damage the row electrodes; the coupling electrodes to the left of the cut line became separated from the touch system. The left half of the LED matrix did not turn on when touching the surface. The right half of smiley face could still be drawn. After heating at 80 °C with a hair drier for 30 s, followed by cooling, the entire smiley face could be drawn again.

CONCLUSIONS

In summary, we have fabricated a transparent and healable touch screen sensor based on a new healable transparent composite electrode material. In this composite electrode, an AgNW percolation network was embedded in an ultrathin layer of a thermally stable polymer, which is bonded to the surface of a healable polymer substrate. As confined by the ultrathin layer, AgNWs enriched along the surface of the composite electrode, resulting in high surface conductivity and reproducible healing. A touch screen sensor comprising 8 row coupling electrodes and 8 column coupling electrodes have been demonstrated using the healable composite electrodes. Each couple of electrodes, with an active electrode and a ground electrode, responded promptly during capacitive changing. A couple of electrodes damaged by razor blade cutting could regain its capacitive sensing function upon heating at 80 °C for 30 s. This cutting-healing could be repeated for up to 4 times. The touch screen sensor integrated into the Arduino microcontroller and LED array should demonstrate the potential applications of this healable touch sensor on various electronic display screens.

METHODS

Synthesis of P(FR-BME). A total of 0.25 g BME was dissolved into 2 mL of cyclopentanone. FR (0.19 g) was then added into the solution, and the mixture was put on test tube rocker until a clear solution was obtained. The solution was drop-cast on a glass substrate and polymerized at 70 °C for 6 h in vacuum.

Preparation of Ultrathin P(PA-FM) Layer. A monomer solution of 5 wt % concentration in cyclopentanone, consisting of PA (CN292, a multifunctional polyester acrylate from Sartomer with excellent wetting property) and FM (furfuryl methacrylate, Sigma-Aldrich) at a weight ratio of 4:1, was spin-coated over the AgNW conductive network at 6,000 rpm, 1 min. The monomer coating was cured under a Dymax ultraviolet bulb, at a speed of 1 foot per minute for one pass. The ultrathin coating was 70 nm thick, as measured by a Dektak profilometer.

Preparation of Transparent Healable AgNW-polymer Composite Film. AgNW was synthesized with an average diameter between 25 and 35 nm, and average length between 10 and 20 μm. A dispersion of AgNW (concentration of 1.5 mg/mL) in isopropanol and methanol (volume ratio, 1:2) was coated on glass substrate using an airbrush (Paasche). Coating ultrathin P(PA-FM) layer over AgNW. Similar to the preparation of P(FR-BME), a solution of BME and FR in cyclopentanone was drop-cast onto the ultrathin P(PA-FM) layer on a glass substrate. The healable comonomers in solution subsequently copolymerized at 70 °C under vacuum for 6 h. The resulting healable composite film was peeled off the glass substrate.

Preparation of Capacitive Touch Screen. A touch screen sensor comprising two composite films patterned as row and column electrodes were overlaid on an LED panel. Each sensing point is upright over an LED. Both the touch screen sensor and LED panel were connected to a programmable control board Arduino Mega 2560, which is powered by a USB cable. The code running on Arduino is available in Support Information.

Characterization Methods. A Keithley 2000 digital multimeter was used to monitor the resistance change. Transmittance spectra were recorded on a Shimadzu UV-1700 spectrophotometer. Scanning electron microscopic images were taken using a JSM-6700F FE-SEM. Cyclic bending-unbending tests were performed on a linear stretcher controlled by a LabView software for automatic recording of bending cycles (Zaber Technologies, Inc.).

Conflict of Interest: The authors declare no competing financial interest.

Acknowledgment. The work reported here was supported by the Air Force Office of Scientific Research (Program Director: Dr. Charles Lee; Grant #FA9550-12-1-0074). J. Li acknowledges support by the China Scholarship Council Program.

Supporting Information Available: Video of healable capacitive touch screen (.avi), and additional results as mentioned in text. This material is available free of charge *via* the Internet at http://pubs.acs.org.

REFERENCES AND NOTES

1. Hecht, D. S.; Hu, L.; Irvin, G. Emerging Transparent Electrodes Based on Thin Films of Carbon Nanotubes, Graphene, and Metallic Nanostructures. *Adv. Mater.* **2011**, *23*, 1482–1513.
2. Cairns, D. R.; Witte, R. P.; Sparacin, D. K.; Sachsman, S. M.; Paine, D. C.; Crawford, G. P.; Newton, R. R. Strain-Dependent

Electrical Resistance of Tin-Doped Indium Oxide on Polymer Substrates. *Appl. Phys. Lett.* **2000**, *76*, 1425–1427.
3. Yuan, W.; Hu, L.; Yu, Z.; Lam, T.; Biggs, J.; Ha, S. M.; Xi, D.; Chen, B.; Senesky, M. K.; Gruner, G.; Pei, Q. Fault-Tolerant Dielectric Elastomer Actuators Using Single-Walled Carbon Nanotube Electrodes. *Adv. Mater.* **2008**, *20*, 621.
4. Li, Y.; Chen, S.; Wu, M.; Sun, J. Polyelectrolyte Multilayers Impart Healability to Highly Electrically Conductive Films. *Adv. Mater.* **2012**, *24*, 4578–4582.
5. Blaiszik, B. J.; Kramer, S. L. B.; Olugebefola, S. C.; Moore, J. S.; Sottos, N. R.; White, S. R. Self-Healing Polymers and Composites. *Annu. Rev. Mater. Res.* **2010**, *40*, 179–211.
6. Wang, Q.; Mynar, J. L.; Yoshida, M.; Lee, E.; Lee, M.; Okuro, K.; Kinbara, K.; Aida, T. High-Water-Content Mouldable Hydrogels by Mixing Clay and a Dendritic Molecular Binder. *Nature* **2010**, *463*, 339–343.
7. White, S. R.; Sottos, N. R.; Geubelle, P. H.; Moore, J. S.; Kessler, M. R.; Sriram, S. R.; Brown, E. N.; Viswanathan, S. Autonomic Healing of Polymer Composites. *Nature* **2001**, *409*, 794–797.
8. Odom, S. A.; Caruso, M. M.; Finke, A. D.; Prokup, A. M.; Ritchey, J. A.; Leonard, J. H.; White, S. R.; Sottos, N. R.; Moore, J. S. Restoration of Conductivity with TTF-TCNQ Charge-Transfer Salts. *Adv. Funct. Mater.* **2010**, *20*, 1721–1727.
9. Chen, X. X.; Dam, M. A.; Ono, K.; Mal, A.; Shen, H. B.; Nutt, S. R.; Sheran, K.; Wudl, F. A Thermally Re-Mendable Cross-Linked Polymeric Material. *Science* **2002**, *295*, 1698–1702.
10. Michal, B. T.; Jaye, C. A.; Spencer, E. J.; Rowan, S. J. Inherently Photohealable and Thermal Shape-Memory Polydisulfide Networks. *ACS Macro Lett.* **2013**, *2*, 694–699.
11. Lu, Y.; Guan, Z. Olefin Metathesis for Effective Polymer Healing *via* Dynamic Exchange of Strong Carbon-Carbon Double Bonds. *J. Am. Chem. Soc.* **2012**, *134*, 14226–14231.
12. Deng, G.; Tang, C.; Li, F.; Jiang, H.; Chen, Y. Covalent Cross-Linked Polymer Gels with Reversible Sol-Gel Transition and Self-Healing Properties. *Macromolecules* **2010**, *43*, 1191–1194.
13. Tee, B. C.; Wang, C.; Allen, R.; Bao, Z. An Electrically and Mechanically Self-Healing Composite with Pressure- and Flexion-Sensitive Properties for Electronic Skin Applications. *Nat. Nanotechnol.* **2012**, *7*, 825–832.
14. Luo, K.; Xie, T.; Rzayev, J. Synthesis of Thermally Degradable Epoxy Adhesives. *J. Polym. Sci., Polym. Chem.* **2013**, *51*, 4992–4997.
15. Yu, S.; Zhang, R.; Wu, Q.; Chen, T.; Sun, P. Bio-Inspired High-Performance and Recyclable Cross-Linked Polymers. *Adv. Mater.* **2013**, *25*, 4912–4917.
16. Pauloehrl, T.; Inglis, A. J.; Barner-Kowollik, C. Reversible Diels-Alder Chemistry as a Modular Polymeric Color Switch. *Adv. Mater.* **2010**, *22*, 2788.
17. Gandini, A. The furan/Maleimide Diels-Alder Reaction: A Versatile Click-Unclick Tool in Macromolecular Synthesis. *Prog. Polym. Sci.* **2013**, *38*, 1–29.
18. Inglis, A. J.; Nebhani, L.; Altintas, O.; Schmidt, F. G.; Barner-Kowollik, C. Rapid Bonding/Debonding on Demand: Reversibly Cross-Linked Functional Polymers *via* Diels-Alder Chemistry. *Macromolecules* **2010**, *43*, 5515–5520.
19. Swanson, J. P.; Rozvadovsky, S.; Seppala, J. E.; Mackay, M. E.; Jensen, R. E.; Costanzo, P. J. Development of Polymeric Phase Change Materials On the Basis of Diels-Alder Chemistry. *Macromolecules* **2010**, *43*, 6135–6141.
20. Wei, H.; Yang, J.; Chu, H.; Yang, Z.; Ma, C.; Yao, K. Diels-Alder Reaction in Water for the Straightforward Preparation of Thermoresponsive Hydrogels. *J. Appl. Polym. Sci.* **2011**, *120*, 974–980.
21. Gong, C.; Liang, J.; Hu, W.; Niu, X.; Ma, S.; Hahn, H. T.; Pei, Q. A Healable, Semitransparent Silver Nanowire-Polymer Composite Conductor. *Adv. Mater.* **2013**, *25*, 4186–4191.
22. Http://arduino.cc/en/Tutorial/CapacitanceMeter.